

Moments of inertia of nuclei in the rare earth region: A relativistic versus nonrelativistic investigation

A. V. Afanasjev,* J. König, and P. Ring

Physik-Department der Technischen Universität München, D-85747 Garching, Germany

L. M. Robledo and J. L. Egido

Departamento de Física Teórica C-XI, Universidad Autónoma de Madrid, E-28049 Madrid, Spain

(Received 7 March 2000; published 10 October 2000)

A parameter-free investigation of the moments of inertia of ground-state rotational bands in well-deformed rare-earth nuclei is carried out using cranked relativistic Hartree-Bogoliubov (CRHB) and nonrelativistic cranked Hartree-Fock-Bogoliubov (CHFb) theories. In CRHB theory, the relativistic fields are determined by the nonlinear Lagrangian with the NL1 force and the pairing interaction by the central part of a finite-range Gogny D1S force. In CHFb theory, the properties in particle-hole and particle-particle channels are defined solely by Gogny D1S forces. Using an approximate particle number projection before variation by means of the Lipkin-Nogami method improves the agreement with the experimental data, especially in CRHB theory. The effect of the particle number projection on the moments of inertia and pairing energies is larger in relativistic than in nonrelativistic theory.

PACS number(s): 21.60.Jz, 27.70.+q

I. INTRODUCTION

One of the oldest problems in our understanding of the collective motion of nuclei is the moments of inertia of ground-state rotational bands in well-deformed nuclei. They depend in a very sensitive way on collective properties such as deformations and on pairing correlations of these many-body systems. Since rotational bands have been detected in nuclei nearly 50 years ago and since the first microscopic calculations of the moments of inertia by Inglis [1], these quantities have been used as a testing ground for nearly all microscopic theories of collective motion. They describe the response of the strongly interacting nuclear many-body system to an external Coriolis field breaking time-reversal symmetry. They are, therefore, in some sense comparable to the static magnetic susceptibility in condensed matter physics.

The earliest microscopic calculations were based on a mean field of a deformed harmonic oscillator [1–3]. In these calculations, residual interactions were neglected. In this way one found the values of the moments of inertia identical to those of a rigid body with the same shape, in strong disagreement with the experimentally observed values, which were considerably smaller. It was pointed out already very early [2,4] that residual two-body interactions would lower the values of the moment of inertia obtained in the Inglis model. The most important correlations causing such a reduction are pairing correlations [5]. In fact, Belyaev [6,7] showed that a simple extension of the Inglis formula in the framework of BCS theory is able to reduce the theoretical moments of inertia dramatically because of the large energy gap in the

spectrum of quasiparticle excitations occurring in the denominator of the Belyaev formula. Therefore, the small moments of inertia of the rotational bands provided one of the most important experimental hints for a superfluid behavior of these heavy open shell nuclei. Extended calculations using the theory of Belyaev have been carried out by Nilsson and Prior [8] using the BCS model based on the single-particle spectrum of the Nilsson potential.

Apart from the fact that the results of these calculations were relatively successful, there are, as we know today, a number of open problems, namely, the following.

(i) Belyaev's formula is based on generalized mean field theory violating essential symmetries. It has been pointed out already by Migdal [9,10] that Galileian invariance is broken. He therefore modified the Belyaev formula by taking into account more complicated correlations to correct the violation of this symmetry. The question of the restoration of the broken Galileian invariance in the particle-hole and particle-particle channels was later discussed in a number of articles; see, for example, Refs. [11–13] and references therein.

(ii) Since Belyaev's formula describes only quasiparticles moving independently, higher order correlations have to be taken into account. This has been done by Thouless and Valatin [14] who considered all orders of the interaction in a theory describing the linear response of the system to the external Coriolis field. Marshalek and Weneser [15] showed that the method of Thouless and Valatin preserves all the symmetries violated in the mean field approximation in linear order. In that sense Migdal's formula was just a special case to deal with Galileian invariance. Marshalek showed in a series of papers (see, for example, Ref. [16]) that this is just the linear approximation of a more general theory based on boson expansion techniques treating the symmetries appropriately in all orders [16].

(iii) Much more elaborated versions of the cranked Nilsson model [17,18] showed that the I^2 term in this model,

*On leave of absence from the Laboratory of Radiation Physics, Institute of Solid State Physics, University of Latvia, LV 2169 Salaspils, Miera str. 31, Latvia.

which corrects in an elegant way the fact that realistic potentials for heavy nuclei are much flatter than an oscillator in the nuclear interior, introduces a strong spurious momentum dependence. This leads to the values for the moments of inertia deviating considerably from the experimental values. However, this problem is to a large extent cured either by Strutinsky renormalization of the moments of inertia [17] or by an additional term to the cranked Nilsson potential that restores the local Galilean invariance [19,20].

Realistic applications of the Thouless-Valatin theory are by no means trivial. They should be based on self-consistent solutions of the mean field equations, because only for those solutions does the random phase approximation (RPA) theory preserve the symmetries [21]. In addition, they require the inversion of the RPA matrix. Meyer *et al.* [22] have carried out such calculations in a restricted configuration space replacing the self-consistent mean field in an approximate way by the Woods-Saxon potential. As the residual interaction they used density-dependent Migdal forces F^ω in the ph channel and F^ξ in the pp channel. These interactions have been carefully adjusted to experimental data for the underlying configuration space. The results of these calculations showed that there are indeed effects originating from both channels, each of them modifying the Belyaev values, but canceling themselves to a large extent. Therefore one could understand why older calculations [8] based on the generalized mean field model gave reasonable results as compared to the experiment.

Nowadays there are theories available where the Hartree-(Fock-)Bogoliubov equations can be solved in a fully self-consistent way in the rotating frame for finite angular velocity Ω . Using the resulting wave functions $|\Phi_\Omega\rangle$ the Thouless-Valatin moment of inertia can be found as

$$J = \frac{d}{d\Omega} \langle \Phi_\Omega | \hat{J}_x | \Phi_\Omega \rangle \Big|_{\Omega=0}. \quad (1)$$

In this way one avoids the inversion of the full RPA matrix, a task which is so far technically impossible for realistic forces in a full configuration space. Among these theories the properties of rotating nuclei are described in a way free from adjustable parameters only in the cranked relativistic Hartree-Bogoliubov (CRHB) theory [23,24] and nonrelativistic density-dependent cranked Hartree-Fock-Bogoliubov (CHFb) theory with finite-range Gogny forces [25,26]. Several realistic investigations of the moments of inertia in normally deformed and in superdeformed bands have been carried out in the literature in the framework of nonrelativistic CHFb theory with Gogny forces [25,27–30]. Similar investigations in the relativistic framework have been performed without pairing in the $A \sim 60$ [31], 80 [32], and 140–150 [33–35] regions of superdeformation where the pairing correlations are expected to be considerably quenched at high spin. The recently developed formalism of the CRHB theory has been applied so far only for the description of the moments of inertia in the $A \sim 190$ mass region of superdeformation [23,24]. A very successful description of the moments of inertia has been obtained in the framework of these two theories. The aim of the present investigation is to find the simi-

larities and differences between these two theories using in a systematic way the moments of inertia of rare-earth nuclei as a testing ground.

II. THEORETICAL TOOLS

CRHB theory [23,24] is an extension of cranked relativistic mean field theory [36,33,34] to the description of pairing correlations in rotating nuclei. It describes the nucleus as a system of Dirac nucleons which interact in a relativistic covariant manner through the exchange of virtual mesons [37]: the isoscalar scalar σ meson, the isoscalar vector ω meson, and the isovector vector ρ meson. The phonon field (A) accounts for the electromagnetic interaction. The CRHB equations for the fermions in the rotating frame are given in a one-dimensional cranking approximation by

$$\begin{pmatrix} \hat{h} - \Omega_x \hat{J}_x & \hat{\Delta} \\ -\hat{\Delta}^* & -\hat{h}^* + \Omega_x \hat{J}_x^* \end{pmatrix} \begin{pmatrix} U_k \\ V_k \end{pmatrix} = E_k \begin{pmatrix} U_k \\ V_k \end{pmatrix}, \quad (2)$$

where $\hat{h} = \hat{h}_D - \lambda$ is the Dirac Hamiltonian \hat{h}_D for the nucleon with mass m ,

$$\hat{h}_D = \boldsymbol{\alpha} [-i\nabla - \mathbf{V}(\mathbf{r})] + V_0(\mathbf{r}) + \beta[m + S(\mathbf{r})], \quad (3)$$

minus the chemical potential λ defined from the average particle number constraint:

$$\langle \Phi_\Omega | \hat{N} | \Phi_\Omega \rangle = N. \quad (4)$$

The Dirac Hamiltonian contains a repulsive vector potential $V_0(\mathbf{r})$, an attractive scalar potential $S(\mathbf{r})$, and the magnetic potential $\mathbf{V}(\mathbf{r})$ which leads to nonvanishing currents in the systems with broken time-reversal symmetries [33,34]. These currents play an extremely important role in the description of the moments of inertia [33,34] and thus they are taken into account fully self-consistently in the calculations. In Eq. (2), U_k and V_k are quasiparticle Dirac spinors and E_k denotes the quasiparticle energies. Furthermore, \hat{J}_x and Ω_x are the projection of total angular momentum on the rotation axis and the rotational frequency.

The time-independent inhomogeneous Klein-Gordon equations for the mesonic fields are given by

$$\{-\Delta - (\Omega_x \hat{L}_x)^2 + m_\sigma^2\} \sigma(\mathbf{r}) = -g_\sigma [\rho_s^p(\mathbf{r}) + \rho_s^n(\mathbf{r})] - g_2 \sigma^2(\mathbf{r}) - g_3 \sigma^3(\mathbf{r}),$$

$$\{-\Delta - (\Omega_x \hat{L}_x)^2 + m_\omega^2\} \omega_0(\mathbf{r}) = g_\omega [\rho_v^p(\mathbf{r}) + \rho_v^n(\mathbf{r})], \quad (5)$$

$$\{-\Delta - [\Omega_x (\hat{L}_x + \hat{S}_x)]^2 + m_\rho^2\} \boldsymbol{\omega}(\mathbf{r}) = g_\omega [\mathbf{j}^p(\mathbf{r}) + \mathbf{j}^n(\mathbf{r})],$$

with source terms involving the various nucleonic densities and currents:

$$\rho_s^i(\mathbf{r}) = \sum_{k>0} [V_k^i(\mathbf{r})]^\dagger \hat{\beta} V_k^i(\mathbf{r}), \quad \rho_v^i(\mathbf{r}) = \sum_{k>0} [V_k^i(\mathbf{r})]^\dagger V_k^i(\mathbf{r}), \quad \kappa \equiv \kappa(\mathbf{r}, s, t, \mathbf{r}', s', t) = \sum_{E_k>0} V_k^*(\mathbf{r}, s, t) U_k(\mathbf{r}', s', t), \quad (8)$$

$$\mathbf{j}^i(\mathbf{r}) = \sum_{k>0} [V_k^i(\mathbf{r})]^\dagger \hat{\mathbf{a}} V_k^i(\mathbf{r}). \quad (6)$$

The sums over $k>0$ run over all quasiparticle states corresponding to positive-energy single-particle states (*no-sea approximation*) and the indices i could be either n (neutrons) or p (protons). For simplicity, the equations for the ρ meson and the Coulomb fields are omitted in Eqs. (5) since they have a structure similar to the equations for ω meson; see Refs. [23,24] for details. Since the coupling constant of the electromagnetic interaction is small compared with the coupling constants of the meson fields, the Coriolis term for the Coulomb potential $A_0(\mathbf{r})$ and the spatial components of the vector potential $\mathbf{A}(\mathbf{r})$ are neglected in the calculations.

The pairing potential Δ in Eq. (2) is given by

$$\Delta \equiv \Delta_{ab} = \frac{1}{2} \sum_{cd} V_{abcd}^{pp} \kappa_{cd}, \quad (7)$$

where the indices a, b, \dots contain the space coordinates \mathbf{r} as well as the Dirac and isospin indices s and t . It contains the pairing tensor κ

and the matrix elements V_{abcd}^{pp} of the effective interaction in the pp channel. In the present version of CRHB theory, pairing correlations are only considered between the baryons, because pairing is a genuine nonrelativistic effect, which plays a role only in the vicinity of the Fermi surface. The central part of the Gogny interaction containing two different finite-range terms [see Eq. (9)] is employed in the pp (pairing) channel.

The CRHB calculations have been performed with the NL1 parametrization [38] of the relativistic mean field (RMF) Lagrangian. The D1S set of parameters [39] is used for the Gogny force in the pairing channel. The CRHB equations are solved in the basis of an anisotropic three-dimensional harmonic oscillator in Cartesian coordinates. A basis deformation of $\beta_0=0.3$ has been used. All fermionic and bosonic states belonging to the shells up to $N_F=13$ and $N_B=16$ are taken into account in the diagonalization and the matrix inversion, respectively. This truncation scheme provides reasonable numerical accuracy for the physical observables which as estimated in the calculations with larger fermionic basis is on the level of $\sim 1.5\%$ or better for kinematic moment of inertia, $J^{(1)}$, and charge quadrupole moments Q_0 . In order to calculate the derivative with respect to Ω in Eq.

TABLE I. The calculated and experimental charge quadrupole moments Q and quadrupole deformation parameters β (shown in square brackets) for typical well-deformed nuclei in the rare-earth region. The results of relativistic calculations are indicated by ‘‘CRHB,’’ while the results of nonrelativistic calculations by ‘‘Gogny.’’ The calculations without and with approximate particle number projection by means of the Lipkin-Nogami method are shown in columns marked by ‘‘Without projection’’ and ‘‘With projection,’’ respectively. The experimental data are taken from Ref. [43].

	Without projection			With projection		Expt.
	A	CRHB	Gogny	CRHB	Gogny	
Gd	154	6.715 [0.335]	6.074 [0.303]	5.907 [0.295]	5.606 [0.280]	6.221 [0.310]
	156	7.199 [0.356]	6.792 [0.336]	6.886 [0.341]	6.601 [0.327]	6.830 [0.338]
	158	7.383 [0.362]	7.077 [0.347]	7.262 [0.356]	6.961 [0.341]	7.104 [0.348]
	160	7.577 [0.369]	7.286 [0.354]	7.490 [0.364]	7.200 [0.350]	7.265 [0.353]
Dy	156	5.860 [0.281]	5.994 [0.287]	5.610 [0.269]	5.438 [0.261]	6.107 [0.293]
	158	7.032 [0.334]	6.990 [0.333]	6.711 [0.319]	6.538 [0.311]	6.844 [0.326]
	160	7.496 [0.354]	7.297 [0.344]	7.373 [0.348]	7.102 [0.335]	7.13 [0.337]
	162	7.711 [0.361]	7.492 [0.350]	7.697 [0.360]	7.382 [0.345]	7.28 [0.341]
	164	7.928 [0.368]	7.626 [0.354]	7.883 [0.366]	7.543 [0.350]	7.503 [0.348]
Er	164	7.671 [0.345]	7.585 [0.341]	7.791 [0.351]	7.522 [0.339]	7.402 [0.333]
	166	8.047 [0.359]	7.781 [0.347]	8.075 [0.361]	7.728 [0.345]	7.656 [0.342]
	168	8.213 [0.364]	7.838 [0.347]	8.151 [0.361]	7.831 [0.347]	7.63 [0.338]
	170	8.137 [0.358]	7.899 [0.347]	8.075 [0.355]	7.782 [0.342]	7.65 [0.336]
Yb	164	6.552 [0.287]	6.900 [0.302]	6.602 [0.289]	6.828 [0.299]	6.60 [0.289]
	166	7.339 [0.318]	7.594 [0.330]	7.653 [0.332]	7.508 [0.326]	7.19 [0.312]
	168	8.362 [0.360]	7.997 [0.344]	8.222 [0.354]	7.864 [0.339]	7.59 [0.327]
	170	8.546 [0.365]	8.147 [0.348]	8.354 [0.357]	8.013 [0.342]	7.57 [0.324]

TABLE II. Pairing energies for typical well-deformed nuclei in the rare-earth region. For details of this table see the caption of Table I.

	A	E_{pair}^n				E_{pair}^p			
		Without projection		With projection		Without projection		With projection	
		CRHB	Gogny	CRHB	Gogny	CRHB	Gogny	CRHB	Gogny
Gd	154	-6.790	-7.413	-11.264	-14.566	-4.556	-8.857	-10.176	-10.828
	156	-6.039	-6.236	-11.552	-12.871	-3.635	-7.740	-8.977	-10.778
	158	-7.071	-6.511	-11.495	-12.355	-3.151	-7.247	-8.748	-10.487
	160	-7.174	-6.731	-11.385	-11.961	-2.579	-6.830	-8.686	-10.341
Dy	156	-5.965	-8.017	-10.904	-15.610	-7.293	-9.849	-11.167	-10.888
	158	-7.007	-8.085	-11.742	-13.870	-5.596	-7.773	-9.888	-11.234
	160	-7.706	-8.067	-11.712	-13.101	-3.077	-6.980	-9.470	-11.090
	162	-6.331	-7.887	-11.440	-12.581	-2.859	-6.323	-9.289	-10.837
	164	-5.237	-6.755	-11.046	-12.169	-3.497	-5.952	-9.187	-10.332
Er	164	-6.154	-8.686	-11.562	-13.157	-5.924	-7.176	-9.938	-11.256
	166	-6.549	-7.520	-11.052	-12.621	-6.019	-6.213	-9.701	-10.603
	168	-4.036	-5.569	-10.784	-12.043	-5.695	-5.555	-9.492	-9.904
	170	-5.741	-4.881	-10.998	-11.58	-4.968	-5.157	-9.289	-9.464
Yb	164	-8.651	-9.462	-12.069	-11.256	-6.388	-9.336	-10.435	-11.708
	166	-7.919	-9.114	-11.527	-10.603	-6.459	-8.223	-10.427	-11.350
	168	-6.702	-7.947	-10.946	-9.904	-6.024	-6.715	-10.12	-10.771
	170	-4.353	-6.061	-10.603	-9.464	-5.274	-5.105	-9.795	-10.051

(1), all CRHB calculations have been performed at rotational frequency $\Omega_x = 0.05$ MeV.

The starting point of the nonrelativistic CHFB theory based on the Gogny force is the phenomenological finite-range two-body interaction of the form [30]

$$\begin{aligned}
V^{pp}(1,2) = & \sum_{i=1,2} e^{-[(r_1-r_2)/\mu_i]^2} (W_i + B_i P^\sigma - H_i P^\tau \\
& - M_i P^\sigma P^\tau) + i W_{LS} [\nabla_{12} \wedge \delta(\mathbf{r}_1 - \mathbf{r}_2) \nabla_{12}] \\
& \times (\boldsymbol{\sigma}_1 + \boldsymbol{\sigma}_2) + t_3 (1 + P^\sigma x_0) \delta(\mathbf{r}_1 - \mathbf{r}_2) [\rho(\mathbf{R})]^{1/3},
\end{aligned} \tag{9}$$

which is used simultaneously both in pp and ph channels. In Eq. (9), $\mathbf{R} = (\mathbf{r}_1 + \mathbf{r}_2)/2$. The transformation to the rotating frame [30] leads to equations similar to Eqs. (2), (7), and (8). The only difference is that the Dirac Hamiltonian of Eq. (3) is replaced by the nonrelativistic Hartree-Fock Hamiltonian h_{ij} containing the density-dependent Gogny force and the rearrangement term $\partial\Gamma_{ij}$, stemming from the density dependence of the force:

$$h_{ij} \rightarrow h_{ij} + \partial\Gamma_{ij} = t_{ij} + \sum_{qq'} \tilde{v}_{iqjq'} \rho_{q'q} + \left\langle \frac{\delta H'}{\delta \rho} f_{ij}(\mathbf{R}) \right\rangle. \tag{10}$$

In the above expression $f_{ij}(\mathbf{r})$ is the quantity appearing in the second-quantization form of the density operator $\rho(\mathbf{r})$

$= \sum_{ij} f_{ij}(\mathbf{r}) c_i^\dagger c_j$. The parameter set D1S [39] has been used in the present calculations. The CHFB equations are again solved in the basis of an anisotropic three-dimensional harmonic oscillator in Cartesian coordinates with the oscillator length $b_0 = 1.98$ fm and the deformation of basis $\beta_0 = 0.3$. Only single-particle states satisfying the condition

$$\hbar \omega_x n_x + \hbar \omega_y n_y + \hbar \omega_z n_z \leq N_{max} \hbar \omega_0 \quad \text{with} \quad N_{max} = 11.1 \tag{11}$$

have been included in the basis. The HFB equation has been solved with the conjugated gradient method [40].

We also consider in this investigation the fluctuations in the pairing field by using the technique of an approximate particle number projection before the variation introduced by Lipkin and Nogami [further APNP(LN)] and discussed in detail in the nonrelativistic case in Refs. [41,42,30]. In the relativistic case, the same approximate particle number projection is used but only the pp part of the interaction is taken into account for the Lipkin-Nogami procedure; see Ref. [24] for details.

III. RESULTS AND DISCUSSION

In order to see the dependence of the results on proton and neutron numbers several nuclei in the Gd, Dy, Er, and Yb isotope chains, the ground-state rotational bands of which are close to rotational limit [$E(4^+)/E(2^+) \approx 3.3$], have been

TABLE III. Moments of inertia $2J^{(1)}$ in units of MeV^{-1} for typical well-deformed nuclei in the rare-earth region. The experimental values are extracted from the energies of the first excited 2^+ states given in Ref. [43]. For other details of this table see caption of Table I.

	Without projection		With projection		Expt.
	A	RHB	Gogny	RHB	
Gd	154	78.19	64.79	49.26	48.75
	156	88.79	78.74	62.15	67.44
	158	86.38	79.05	66.42	75.46
	160	87.30	81.56	68.80	79.72
Dy	156	63.22	57.52	43.32	47.79
	158	80.45	72.81	56.17	60.64
	160	93.76	76.14	63.71	67.38
	162	98.22	77.56	67.24	74.38
	164	99.92	82.41	69.80	81.75
Er	164	88.49	72.50	64.73	65.65
	166	83.34	76.40	68.20	74.46
	168	93.74	82.19	69.04	75.19
	170	82.30	81.08	67.39	76.25
	Yb	164	61.66	60.72	49.88
166		70.54	67.72	61.24	58.61
168		82.96	75.00	67.37	68.39
170		93.12	80.53	68.61	71.21

selected for the present study. The results of relativistic and nonrelativistic calculations with and without the APNP(LN) method are presented in Tables I–III and Figs. 1 and 2 and compared with the experiment. Such quantities as charge quadrupole moments (deformations), pairing energies, and moments of inertia are discussed below.

The calculated and experimental charge quadrupole moments Q and quadrupole deformation parameters β derived from Q by

$$Q = \sqrt{\frac{16\pi}{5}} \frac{3}{4\pi} ZR_0^2\beta \quad \text{where} \quad R_0 = 1.2A^{1/3} \quad (12)$$

are shown in Table I and Fig. 1. The general feature is that the charge quadrupole moments Q obtained in relativistic calculations are larger than the ones of the nonrelativistic calculations. In the nonrelativistic case, the Q values calculated with the APNP(LN) method are slightly smaller than the ones obtained without the APNP(LN) method because of the larger pairing correlations (see Table II), which in general favors more spherical configurations. This trend also persists in the relativistic case, but there are the cases ($^{164,166}\text{Er}$, $^{164,166}\text{Yb}$) in which the APNP(LN) method leads to larger charge quadrupole moments as compared with unprojected calculations. As shown in Fig. 1, the nonrelativistic results are somewhat closer to the experiment than the relativistic ones. However, considering that the experimental

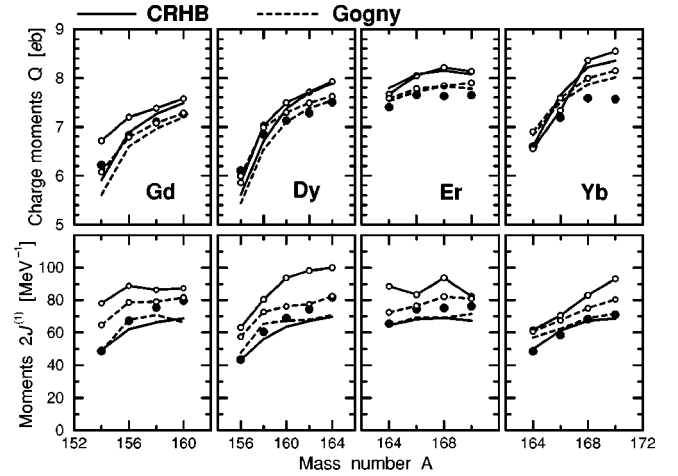


FIG. 1. Experimental and calculated charge quadrupole moments Q (top panels) and moments of inertia $2J^{(1)}$ (bottom panels) of well-deformed rare-earth nuclei. The experimental data are shown by solid unlinked circles. The results of calculations with the APNP(LN) method are shown by the lines without symbols. The lines with open symbols are used to indicate the results of calculations without the APNP(LN) method. Solid and dashed lines are used for relativistic and nonrelativistic results, respectively.

values of Q are the subject of considerable experimental errors [43], one can conclude that both theories describe experimental charge quadrupole moments reasonably well which allows us to proceed further with the study of more sensitive quantities such as moments of inertia.

In Hartree-(Fock-)Bogoliubov calculations the size of the pairing correlations is usually measured in terms of the pairing energy defined as

$$E_{pair} = -\frac{1}{2}\text{Tr}(\Delta\kappa). \quad (13)$$

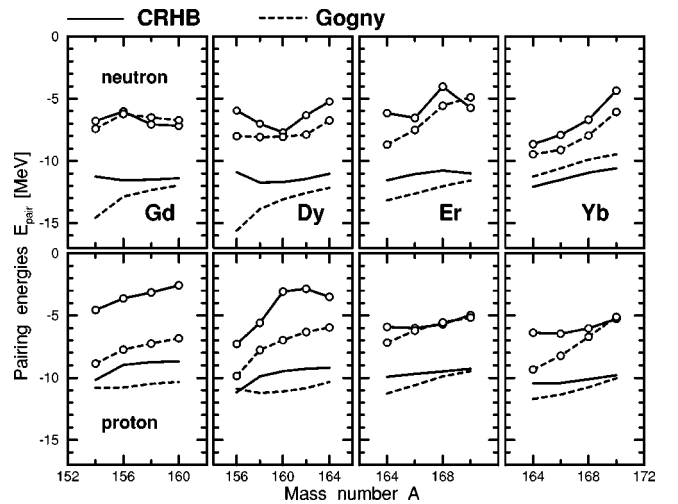


FIG. 2. Calculated neutron (top panels) and proton (bottom panels) pairing energies. The results of calculations with (without) the APNP(LN) method are shown by the lines without (with) symbols. Solid and dashed lines are used for relativistic and nonrelativistic results, respectively.

This is not an experimentally accessible quantity, but it is a measure for the size of the pairing correlations in the theoretical calculations. These quantities are shown in Table II and Fig. 2 for protons and neutrons separately. Both in relativistic and nonrelativistic calculations, we observe that the APNP(LN) method leads to an increase of the pairing energies. This increase shows large variations as a function of the proton and neutron numbers. In general, this increase is larger in relativistic calculations. For example, proton pairing energies increase on average by a factor of 2.16 [with minimal and maximal increases being equal to 1.53 (^{156}Dy) and 3.36 (^{160}Gd)]. In nonrelativistic calculations, the average increase of proton pairing energies is only 1.55 [with minimal and maximal increases being equal to 1.11 (^{156}Dy) and 1.97 (^{170}Yb)]. Neutron pairing energies behave in a similar way but there the difference between relativistic and nonrelativistic calculations is smaller: the average increase of neutron pairing energies due to the APNP(LN) method is 1.81 in the relativistic and 1.73 in the nonrelativistic calculations. In some cases, such as, for example, in the Gd isotopes, the increase of neutron pairing energies due to the APNP(LN) method is larger in nonrelativistic calculations. This increase of pairing energies due to the APNP(LN) method will lead to an increase of the pairing gaps, as is well known from many phenomenological calculations using the monopole pairing force [44,45]. We also see that with few exceptions the pairing energies are smaller in relativistic calculations. An additional effect of the APNP(LN) method is the increase of absolute values of binding energies. In relativistic calculations, the APNP(LN) method provides an additional binding by ≈ -2.5 MeV.

Calculated moments of inertia are given in Table III and Fig. 1. Comparing the results of calculations without the APNP(LN) method, it is clear that the moments of inertia are systematically larger in the relativistic case. Although one cannot completely exclude that this feature is to some extent connected with a different angular momentum content of single-particle orbitals in relativistic and nonrelativistic calculations, a detailed analysis of pairing energies and moments of inertia suggests that this fact can be explained in a more realistic way by the different effective masses of the two theories: $m^*/m \sim 0.6$ in RMF theory and ~ 0.7 in the nonrelativistic theory. Thus the corresponding level density in the vicinity of the Fermi level is smaller in the relativistic theory which in general leads to weaker pairing correlations (see Table II and discussion above) as compared with nonrelativistic calculations and as a result to larger moments of

inertia. The APNP(LN) method restores to a large extent the correct size of pairing correlations and thus its effect is larger in relativistic calculations. The average decrease of the moments of inertia due to the APNP(LN) method over the considered set of nuclei is 1.35 and 1.15 in relativistic and nonrelativistic calculations, respectively. It is also clearly seen that the APNP(LN) method improves on average and especially in the relativistic case the agreement between experimental and calculated moments of inertia. The level of agreement between calculations with the APNP(LN) method and experiment is similar in both theories; however, some discrepancies still remain.

IV. CONCLUSIONS

In conclusion, the moments of inertia, charge quadrupole moments, and pairing energies of well-deformed nuclei in the rare-earth region have been investigated within relativistic and nonrelativistic mean field theories with and without approximate particle number projection by means of the Lipkin-Nogami method. With no adjustable parameters it was possible to obtain a good description of the experimental data. It was found that particle number projection plays a more important role in the relativistic calculations, most likely reflecting the lower effective mass. In addition, it has a larger impact on the moments of inertia and the pairing energies as compared with the charge quadrupole moments. The remaining deviations from experimental data could be related either to the parametrization of the mean field or to the interaction in the pairing channel or to the approximate character of the particle number projection. Further and more systematic investigations are needed for clarification of the main source of discrepancies between theory and experiment.

ACKNOWLEDGMENTS

A.V.A. acknowledges support from the Alexander von Humboldt Foundation. This work has been supported in part by DGICYT, Spain, under Project No. PB97-0023 and the Bundesministerium für Bildung und Forschung under Project No. 06 TM 875. P.R. wishes to express his gratitude to the Spanish Ministry for Education for support of his work at the Universidad Autónoma de Madrid in the framework of the A. von Humboldt–J.C. Mutis program for the Scientific Cooperation between Spain and Germany.

-
- [1] D. R. Inglis, *Phys. Rev.* **96**, 1059 (1954).
 [2] A. Bohr and B. R. Mottelson, *Mat. Fys. Medd. K. Dan. Vidensk. Selsk.* **30**, 1 (1955).
 [3] D. R. Inglis, *Phys. Rev.* **103**, 1786 (1956).
 [4] S. A. Moszkowski, *Phys. Rev.* **103**, 1328 (1956).
 [5] A. Bohr, B. R. Mottelson, and D. Pines, *Phys. Rev.* **110**, 936 (1958).
 [6] S. T. Belyaev, *Mat. Fys. Medd. K. Dan. Vidensk. Selsk.*

- 3** (11), 1 (1959).
 [7] S. T. Belyaev, *Nucl. Phys.* **24**, 322 (1961).
 [8] S. G. Nilsson and O. Prior, *Mat. Fys. Medd. K. Dan. Vidensk. Selsk.* **32** (16), 1 (1961).
 [9] A. B. Migdal, *Nucl. Phys.* **13**, 655 (1959).
 [10] A. B. Migdal, *Zh. Éksp. Teor. Fiz.* **37**, 249 (1960) [*Sov. Phys. JETP* **10**, 176 (1960)].
 [11] S. T. Belyaev, *Phys. Lett.* **28B**, 365 (1969).

- [12] H. Sakamoto and T. Kishimoto, Phys. Lett. B **245**, 321 (1990).
- [13] T. Kubo, H. Sakamoto, T. Kammuri, and T. Kishimoto, Phys. Rev. C **54**, 2331 (1996).
- [14] D. J. Thouless and J. G. Valatin, Nucl. Phys. **31**, 211 (1962).
- [15] E. R. Marshalek and J. Weneser, Phys. Rev. C **2**, 1682 (1970).
- [16] E. R. Marshalek, Phys. Rev. C **35**, 1900 (1987).
- [17] G. Andersson, S. E. Larsson, G. Leander, P. Möller, S. G. Nilsson, I. Ragnarsson, S. Åberg, R. Bengtsson, J. Dudek, B. Nerlo-Pomorska, K. Pomorski, and Z. Szymański, Nucl. Phys. **A268**, 205 (1976).
- [18] K. Neergård, V. V. Pashkevich, and S. Frauendorf, Nucl. Phys. **A262**, 61 (1976).
- [19] A. Bohr and B. R. Mottelson, *Nuclear Structure* (Benjamin, New York, 1975), Vol. 2.
- [20] T. Nakatsukasa, K. Matsuyanagi, S. Mizutori, and Y. R. Shimizu, Phys. Rev. C **53**, 2213 (1996).
- [21] P. Ring and P. Schuck, *The Nuclear Many-Body Problem* (Springer-Verlag, Heidelberg, 1980).
- [22] J. Meyer, J. Speth, and J. H. Vogeler, Nucl. Phys. **A193**, 60 (1972).
- [23] A. V. Afanasjev, J. König, and P. Ring, Phys. Rev. C **60**, 051303 (1999).
- [24] A. V. Afanasjev, P. Ring, and J. König, Nucl. Phys. **A676**, 196 (2000).
- [25] J. L. Egido and L. Robledo, Phys. Rev. Lett. **70**, 2876 (1993).
- [26] M. Girod, J. P. Delaroche, J. F. Berger, and J. Libert, Phys. Lett. B **325**, 1 (1994).
- [27] J. L. Egido and L. M. Robledo, Nucl. Phys. **A570**, 69c (1994).
- [28] A. Valor, J. L. Egido, and L. M. Robledo, Phys. Lett. B **392**, 249 (1997).
- [29] A. Villafranca and J. L. Egido, Phys. Lett. B **408**, 35 (1997).
- [30] A. Valor, J. L. Egido, and L. M. Robledo, Nucl. Phys. **A665**, 46 (2000).
- [31] A. V. Afanasjev, I. Ragnarsson, and P. Ring, Phys. Rev. C **59**, 3166 (1999).
- [32] A. V. Afanasjev, J. König, and P. Ring, Phys. Lett. B **367**, 11 (1996).
- [33] J. König and P. Ring, Phys. Rev. Lett. **71**, 3079 (1993).
- [34] A. V. Afanasjev, J. König, and P. Ring, Nucl. Phys. **A608**, 107 (1996).
- [35] A. V. Afanasjev, G. A. Lalazissis, and P. Ring, Nucl. Phys. **A634**, 395 (1998).
- [36] W. Koepf and P. Ring, Nucl. Phys. **A493**, 61 (1989).
- [37] B. D. Serot and J. D. Walecka, Adv. Nucl. Phys. **16**, 1 (1986).
- [38] P. G. Reinhard, M. Rufa, J. Maruhn, W. Greiner, and J. Friedrich, Z. Phys. A **323**, 13 (1986).
- [39] J. F. Berger, M. Girod, and D. Gogny, Nucl. Phys. **A428**, 23c (1984).
- [40] J. L. Egido, J. Lessing, V. Martin, and L. M. Robledo, Nucl. Phys. **A594**, 70 (1995).
- [41] B. Gall, P. Bonche, J. Dobaczewski, H. Flocard, and P.-H. Heenen, Z. Phys. A **348**, 183 (1994).
- [42] W. Satuła, R. Wyss, and P. Magierski, Nucl. Phys. **A578**, 45 (1994).
- [43] S. Raman, C. H. Malarkey, W. T. Milner, C. W. Nestor, Jr., and P. H. Stelson, At. Data Nucl. Data Tables **36**, 1 (1987).
- [44] J. L. Egido and P. Ring, Nucl. Phys. **A383**, 189 (1982).
- [45] J. L. Egido and P. Ring, Nucl. Phys. **A388**, 19 (1982).